

Workspace Analysis of a 6-DOF Cable Robot for Hardware-in-the-Loop Dynamic Simulation

Xiumin Diao

Department of Mechanical Engineering
 New Mexico State University
 Las Cruces, NM, USA 88003
 xiumin@nmsu.edu

Ou Ma

Department of Mechanical Engineering
 New Mexico State University
 Las Cruces, NM, USA 88003
 oma@nmsu.edu

Abstract - This paper describes the study of the force-closure workspace of a 6-DOF, cable-driven, parallel robot for the application in a hardware-in-the-loop dynamic simulator, which is used for simulating microgravity contact dynamics of spacecraft or robotic systems. The workspace under study is defined as the set of all end-effector poses satisfying force-closure condition. Force-closure also means that the inverse dynamics problem of the manipulator has a feasible solution. Since there is no limitation on the external wrench and the dynamic motion of the end-effector, such a workspace is the most desirable (or non-restricted) workspace for the intended application – simulating low-speed impact-contact dynamics. A systematic method of determining whether or not a given end-effector's pose is inside the workspace is proposed with mathematical proof. Based on this method, the shape, boundary, dimensions, and volume of the workspace of a 6-DOF cable robot are displayed and discussed.

Index Terms - Cable robot, wire robot, force-closure, workspace, hardware-in-the-loop simulator.

I. INTRODUCTION

Ground-based test and verification of dynamic response to arbitrary physical contact in space environment is extremely difficult. The existing ground-based zero-g test technologies have difficulties to representatively test full 6-DOF microgravity contact dynamics of large and complex space systems. Robotics-based active gravity compensation systems allow simulation and test of a complex space system under fully 6-DOF dynamic motion. Plus, it can use physical contact test to generate contact forces and thus it is more accurate than any contact-dynamics mathematical model. The concept of such a robot-based, contact-dynamics test facilitate is illustrated in Fig. 1. Such a system is, in fact, a hardware-in-the-loop (HIL) active dynamic simulator, combining both software and hardware simulations in an integrated framework and taking advantages of both. It consists of three basic parts:

- 1) a real-time computer simulator to predict dynamic response of the simulated space system such as a spacecraft or robot, based on its dynamics model;
- 2) a 6-DOF robotic manipulator to physically deliver the computer-generated dynamic motion of the simulated space system; and
- 3) a physical mockup of the contact interface or environment to allow real physical contact of the simulated system.

In this concept, the dynamics of a spacecraft including the microgravity condition is predicted by computer simulation

because it is very difficult to experimentally produce a full 6-DOF on-orbit dynamic motion on the ground but easy to model and simulate such dynamics on a computer. On the other hand, contact with the complicated environment is represented by real physical contact because such contact action is very difficult to model in mathematics and simulate on computers.

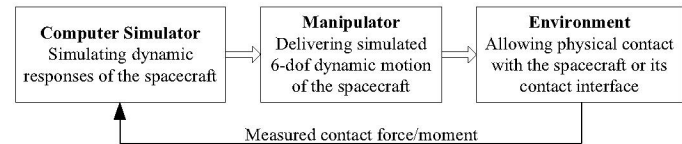


Fig. 1 Three parts of an HIL contact-dynamics simulator

There have been several examples of HIL simulators for simulating microgravity dynamics. NASA developed an HIL simulator using a Stewart platform for simulating the space shuttle berthing to the International Space Station [1]. The Canadian Space Agency (CSA) built a SPDM Task Verification Facility using a serial-type hydraulic manipulator to simulate SPDM contact tasks [2]. SPDM is a two-arm space robot developed by CSA for the assembly and maintenance of the International Space Station. German Space Agency (DLR) also investigated a similar simulator earlier [3]. All the three systems experienced a common technical difficulty: the manipulator used to deliver the dynamic motion of the simulated space system is too complicated so that the manipulator's own dynamics cannot be accurately predicted and compensated, which, in turn, reduces the fidelity of the facility. To overcome this technical difficulty, a new HIL system was proposed, as shown in Fig. 2. The manipulator used in this new system is a cable-driven parallel robot. Unlike the Stewart platform such as the one used in [1] and other rigid-link serial robots such as the one used in [2, 3], the cable robot has a much simpler dynamics model because: (1) its cable “links” have negligible inertia compared to its end-effector and thus, the inertia forces and moments of all the links can be ignored; (2) the force in each cable is 1-dimensional only while a rigid link must have a 3-D force plus a 3-D moment instead. As a result, the robot's own dynamics can be accurately predicted and then compensated, which is the most critical requirement for such an HIL simulator.

The design of the cable robot under study is shown in Fig. 2, which is driven by seven cables. Compared to most of the cable robots such as those studied in [4-9], this type of design

does not have the potential problem of cable interference (due to its special cable arrangement) and, therefore, it can fully take advantage of redundant drive (i.e., having more than necessary number of cables) for performance optimization. The feasibility of such a cable-robot based HIL simulator will rely on several factors. One of the most critical factors is how large its workspace is for a given design. In a contact dynamics simulation, the cable robot has to speed up the tested mechanical object from still to a required velocity and then maintain that velocity in steady-state before a specific contact simulation can meaningfully start. Such an accelerating and subsequently velocity-holding procedure requires a sizeable physical space and this physical space must be within the feasible workspace of the robot. Thus, the designer of the robot has to know how to determine the workspace of a robot in order to have it meet the design requirements of the HIL simulator. Similarly, the user of such a simulator also has to have knowledge of the workspace (such as its topologic shape, geometric dimensions, location and orientation, etc.) in order to properly use the simulator. Therefore, a practical and easy-to-use method of determining the feasible workspace of such a cable robot is needed.

Workspace analysis of cable driven robots is still an active research topic. In general, a workspace of a cable robot is defined as the set of all poses (positions and orientations) at which the end-effector can physically reach with: 1) all the cables are in tension and 2) all other specific motion and/or force constraints are satisfied. The second condition leads to different types of workspace discussed in the literature. Verhoeven and Hiller studied the *controllable workspace*, which is defined as the set of all the poses at which the end-effector can statically balance a specific set of external wrench with all-positive cable forces [4]. Bartette and Gosselin introduced the concept of *dynamic workspace*, which is defined as the set of all end-effector poses and accelerations at which the end-effector can be balanced with all-positive cable forces. Apparently, it is a workspace defined in a mixed space of end-effector pose and acceleration. Ebert-Uphoff et al. proposed the concept of wrench set, which is defined as the set of all external wrenches corresponding to a set of specific limits of cable forces [6, 7]. They applied the wrench set theory to a *wrench-feasible workspace* defined as the set of all the poses which can balance a specified range of external wrench. Fattah and Agrawal [8] studied the *static workspace* of a 6-6 cable robot. A static workspace is defined as the set of all the poses at which the end-effector can be statically balanced with all-positive cable forces. Williams II et al. also studied the static workspace of a 6-cable robot for sculpture surface metrology [9].

The workspace discussed in this paper is termed as *force-closure workspace*, which is defined as the set of all the poses satisfying the force-closure condition and similar as the workspace discussed in [11] for planar robots. Since a force-closure workspace is defined without any constraints on the external wrench and end-effector acceleration, for any poses in it, the end-effector can balance any external wrench and

undergo any acceleration by all-positive cable forces. Hence, a force-closure workspace is most desirable for the intended application because, during a physical impact-contact test, the resulting contact wrench and the impact motion are very unpredictable. Note that, this type of workspace, by definition, does not contain any singular loci. Although such a definition of workspace does not limit cable forces and accelerations, it is important for the theoretical design and analysis of cable manipulators. It should be emphasized that in practice force limits of cables and driving joints will limit the external wrench which can actually be applied.

II. THE CABLE-DRIVEN PARALLEL ROBOT

The 6-DOF cable robot under study along with its potential application in an HIL simulator is illustrated in Fig. 2. The end-effector (moving platform) of the robot is controlled by seven cables with their driving actuators mounted to the fixed base. The purpose of using seven cables as opposed to six is to enable the cables in tension during operation [10]. The number of cables can be more than seven in the design.

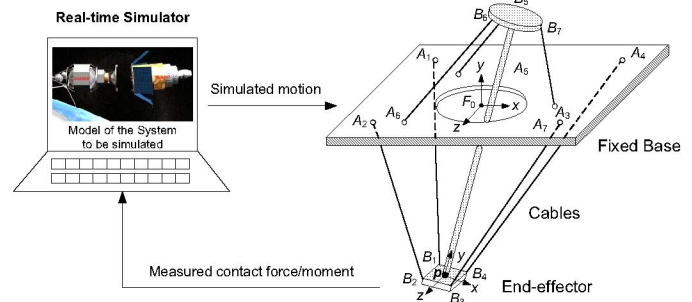


Fig. 2 Six-DOF HIL microgravity contact-dynamics simulator

Cable robots have several advantages over rigid-link manipulators. First, they can have larger workspaces because their joints can reel out a large amount of cables. Second, all of their actuators and transmission systems can be mounted on the fixed base and thus, they have a higher payload-to-weight ratio, which makes them attractive for high-load and high-speed applications. Third, their special designs make them potentially inexpensive, modular, and very easy to reconfigure. Finally, and also the most important for HIL simulation, they have much simpler dynamics model than their rigid-link counterparts because the inertias of their links (i.e., cables) can be ignored.

This type of cable robots has been studied for simulation [12] and for hepatic human-machine interface [13]. The research in [12] focused on vibration analysis. Although the authors of [13] pointed out that the positive cables forces can be obtained if the columns of the Jacobian matrix satisfying the vector-closure condition [14], they missed a key step that is to mathematically show the relationship between the vector-closure condition and the specific design and end-effector pose of such a robot. In other word, a systematic method of determining whether the vector-closure condition is met needs to be addressed, which is the topic of this paper.

III. MODELING AND WORKSPACE DEFINITION

The kinematic notation of a 7-cable robot is defined in Fig. 3, where \mathbf{q}_i , for $i = 1, 2, \dots, 7$, is the vector along the i th cable and has the same length as the cable. The length of the i th cable is represented by the robot's joint variable q_i . \mathbf{u}_i is the unit vector along the i th cable. A_i and B_i are the two attaching points of the i th cable on the base and the end-effector, respectively. The positions of the two attaching points are represented by vectors \mathbf{a}_i and \mathbf{b}_i , respectively. Obviously, \mathbf{a}_i is a constant vector in the base frame F_0 and \mathbf{b}_i is a constant vector in the end-effector frame F_e . Based on the kinematics notation, the position of the end-effector (referred to by a reference point P on the end-effector) can be described as

$$\mathbf{p} = \mathbf{a}_i - \mathbf{q}_i - \mathbf{b}_i \quad \text{for } i = 1, 2, \dots, 7 \quad (1)$$

from which one has

$$q_i^2 = [\mathbf{a}_i - \mathbf{p} - \mathbf{b}_i]^T [\mathbf{a}_i - \mathbf{p} - \mathbf{b}_i] \quad \text{for } i = 1, 2, \dots, 7 \quad (2)$$

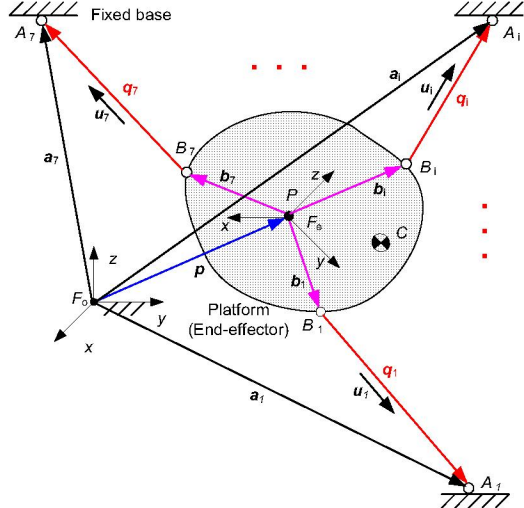


Fig. 3 Kinematics notation of a 6-DOF 7-cable manipulator

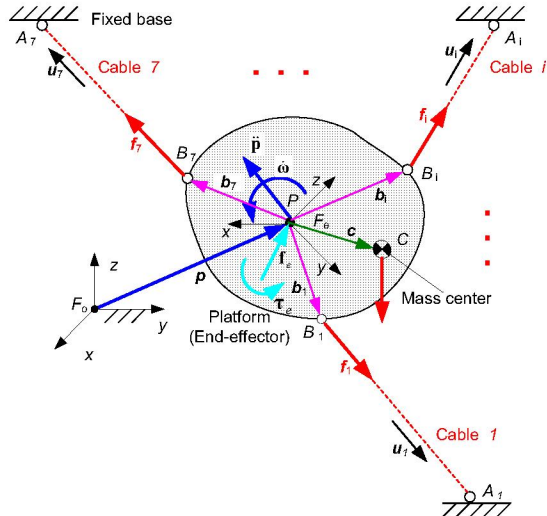


Fig. 4 Dynamics notation of a 6-DOF 7-cable manipulator

Differentiating (2) with respect to time, and then assembling the seven resulting equations into matrix form, one obtains

$$\dot{\mathbf{q}} = \mathbf{J}\mathbf{t} \quad (3)$$

where

$$\dot{\mathbf{q}} = [\dot{q}_1 \ \dot{q}_2 \ \dots \ \dot{q}_7]^T, \mathbf{J} = \begin{bmatrix} \mathbf{u}_1 & \mathbf{u}_2 & \dots & \mathbf{u}_7 \\ \mathbf{b}_1 \times \mathbf{u}_1 & \mathbf{b}_2 \times \mathbf{u}_2 & \dots & \mathbf{b}_7 \times \mathbf{u}_7 \end{bmatrix}^T \quad (4)$$

$$\mathbf{t} = \begin{bmatrix} \dot{\mathbf{p}} \\ \boldsymbol{\omega} \end{bmatrix} = [\dot{x} \ \dot{y} \ \dot{z} \ \omega_x \ \omega_y \ \omega_z]^T \quad (5)$$

where $\dot{\mathbf{p}}$ is the velocity vector of reference point P ; $\boldsymbol{\omega}$ is the angular velocity vector of the end-effector; and \mathbf{t} represents the twist vector in R^6 which includes both the linear and angular velocities of the end-effector. Apparently, \mathbf{J} is the 7×6 Jacobian matrix corresponding to this parallel robot.

For this type of robots, the inertia of each link is negligible compared to that of the end-effector because the so-called link is just a cable. Therefore, one can ignore the dynamics of the links, which will significantly simplify the dynamics model of the robot. Based upon the dynamics notation in Fig. 4, one can derive the Newton-Euler equations of motion of the robot with respect to the point P as follows

$$\mathbf{J}^T \mathbf{f} = \mathbf{w}_e + \mathbf{w}_g - \mathbf{M}\dot{\mathbf{t}} - \mathbf{N}\mathbf{t} \quad (6)$$

which can be re-written into a compact form as

$$\mathbf{A}\mathbf{f} = \mathbf{w} \quad (7)$$

where

$$\begin{aligned} \mathbf{A} &\equiv \mathbf{J}^T, & \mathbf{w} &\equiv \mathbf{w}_e + \mathbf{w}_g - \mathbf{M}\dot{\mathbf{t}} - \mathbf{N}\mathbf{t} \\ \mathbf{M} &\equiv \begin{bmatrix} m\mathbf{1} & -m\mathbf{c}^\times \\ m\mathbf{c}^\times & \mathbf{I} \end{bmatrix}, & \mathbf{N} &\equiv \begin{bmatrix} \mathbf{0} & -m(\boldsymbol{\omega} \times \mathbf{c})^\times \\ m(\boldsymbol{\omega} \times \mathbf{c})^\times & -(\mathbf{I}\mathbf{c})^\times \end{bmatrix} \\ \mathbf{f} &\equiv [f_1 \ f_2 \ \dots \ f_7]^T, & \mathbf{w}_e &\equiv \begin{bmatrix} \mathbf{f}_e \\ \boldsymbol{\tau}_e \end{bmatrix}, \quad \mathbf{w}_g \equiv \begin{bmatrix} mg \\ \mathbf{c} \times mg \end{bmatrix} \end{aligned} \quad (8)$$

Where \mathbf{f} is a 7-D vector consisting of the force value of each cable. f_i is the force value of the i th cable. When the i th cable is in tension, f_i is positive. \mathbf{w}_e and \mathbf{w}_g are the 6-D external and gravity wrenches exerted on the reference point P of the end-effector; \mathbf{f}_e and $\boldsymbol{\tau}_e$ are 3-D external force and moment applied to the end-effector about reference point P ; m is the mass of the end-effector including any attached payload; \mathbf{I} is the 3×3 inertia tensor of the end-effector about the reference point P ; \mathbf{g} is the 3-D gravity acceleration vector; In addition, $\mathbf{0}$ and $\mathbf{1}$ are the 3×3 zero matrix and identity matrix, respectively; \mathbf{c} is the 3-D position vector of the mass center of the end-effector with respect to the reference point P ; and $(\cdot)^\times$ is the operator for cross product $(\cdot) \times$.

Definition 1: The force-closure workspace is defined as the entire set of $\mathbf{x} = [x, y, z, \theta_x, \theta_y, \theta_z]^T$, where θ_x, θ_y and θ_z are a set of Euler angles, satisfying

$$\forall \mathbf{w} \in R^6, \exists \mathbf{f} > 0, \exists \mathbf{A}\mathbf{f} = \mathbf{w} \quad (9)$$

Since the 6-D vector \mathbf{w} is the resultant wrench of all the inertia wrenches of the end-effector and all the external

wrenches exerted on the end-effector, it is clear that the workspace defined here is the entire set of end-effector poses which can generate any specified dynamic motion (represented by \mathbf{t} and $\dot{\mathbf{t}}$) under any given external wrench (represented by \mathbf{w}_e) while all the individual cable forces (represented by f_i 's) are positive. Because of no restrictions on the external wrench and the end-effector's acceleration, this workspace, if made known to the user, is the most desirable workspace for the intended application among all the static and dynamic workspaces summarized in Section I.

IV. WORKSPACE DETERMINATION

A few researchers have pointed out that the force feasibility problem of cable robots is mathematically equivalent to the frictionless multi-finger rigid-body grasping problem. In the former, all the cables must be in tension while in the latter all the fingers must be in compression. The grasping problem has been extensively studied in 80's and 90's of the last century. The most cited approaches for solving the grasping problem is based on the vector-closure and convexity theories [14, 15]. Some researchers proposed force/workspace analyses based on the analog between cable robots and multi-finger hands [6, 13, 16]. To avoid the burden of rigorously proving such an analog, we introduce a systematic method of determining workspace without referring to any techniques specifically developed for the multi-finger grasping problem. The method consists of the following four steps:

- 1) Select any set of six linearly independent column vectors of matrix \mathbf{A} to form a new 6×6 matrix $\hat{\mathbf{A}}$. This is always possible as long as \mathbf{A} has full rank. Without loss of generality, let us assume $\hat{\mathbf{A}} = [\mathbf{a}_1, \mathbf{a}_2, \dots, \mathbf{a}_6]$.
- 2) Define a 6×6 matrix $\mathbf{V} = [\mathbf{v}_1, \mathbf{v}_2, \dots, \mathbf{v}_6]$ such that $\mathbf{V}^T = \hat{\mathbf{A}}^{-1}$. This is always feasible because all of the columns of $\hat{\mathbf{A}}$ are linearly independent by definition.
- 3) Pre-multiply the remaining column of \mathbf{A} by \mathbf{V}^T , i.e.,

$$\mathbf{V}^T \mathbf{a}_7 = \begin{bmatrix} \mathbf{v}_1^T \mathbf{a}_7 \\ \mathbf{v}_2^T \mathbf{a}_7 \\ \vdots \\ \mathbf{v}_6^T \mathbf{a}_7 \end{bmatrix}, \text{ if } \hat{\mathbf{A}} = [\mathbf{a}_1, \mathbf{a}_2, \dots, \mathbf{a}_6] \quad (10)$$

- 4) Check the signs of the components of vector $\mathbf{V}^T \mathbf{a}_7$. If all the nonzero components are negative, then the force-closure condition is met or all the cable forces solved from (7) are positive. Otherwise, the force-closure condition is not met.

The improvements of this method over that described in [16-18] are: a) the procedure is more straightforward; b) only one vector needs to be formed and checked while the method in [16-18] requires to check 21 (i.e., C_7^5) vectors instead; moreover, no proof is given in both references that the examination of the sign condition of the 21 \mathbf{v} vectors will meet the sufficient condition of the force-closure theorem,

which requires that each and every $\mathbf{v} \in R^6$ has to satisfy the sign condition. The following is a proof of the proposed method for verifying the force-closure condition.

Proof of sufficient condition:

Equation (9) can be re-written as

$$\hat{\mathbf{A}}\hat{\mathbf{f}} + \mathbf{a}_7 f_7 = \mathbf{w} \quad (11)$$

where $\hat{\mathbf{f}} = [f_1 \ f_2 \ \dots \ f_6]^T$ and f_i ($i = 1, 2, \dots, 7$) are components of vector \mathbf{f} . From (11), for any $\mathbf{w} \in R^6$, one has

$$\hat{\mathbf{f}} = \hat{\mathbf{A}}^{-1}\mathbf{w} - \hat{\mathbf{A}}^{-1}\mathbf{a}_7 f_7 = \mathbf{V}^T \mathbf{w} - \mathbf{V}^T \mathbf{a}_7 f_7 > \mathbf{0} \quad (12)$$

This is because all the components of $\mathbf{V}^T \mathbf{a}_7$ are negative and f_7 is a positive number and hence, each component of $-\mathbf{V}^T \mathbf{a}_7 f_7$ is a positive number and it can always be made larger than the absolute value of the corresponding component of $\mathbf{V}^T \mathbf{w}$ by properly choosing an f_7 . In this case, f_7 can be arbitrarily chosen as long as it is positive. This completes the proof of sufficient condition.

Proof of necessary condition:

The necessary condition can be easily shown by disproving that, when $\mathbf{f} > \mathbf{0}$ or (12) holds, it is impossible to have some of the components of $\mathbf{V}^T \mathbf{a}_7$ positive. Assume that vector $\mathbf{V}^T \mathbf{a}_7$ has one or more positive components. Since \mathbf{w} is arbitrary in R^6 , let $\mathbf{w} = -\mathbf{a}_7 f_7$. This leads to

$$\hat{\mathbf{f}} = \mathbf{V}^T \mathbf{w} - \mathbf{V}^T \mathbf{a}_7 f_7 = -2\mathbf{V}^T \mathbf{a}_7 f_7 \quad (13)$$

which obviously has one or more negative components because f_7 is a positive number. This contradicts the assumption of $\mathbf{f} > \mathbf{0}$ and hence, $\mathbf{V}^T \mathbf{a}_7$ cannot have even one positive component. This proves the necessary condition.

V. NUMERICAL EXAMPLE

For illustration of the workspace, a numerical example of a cable manipulator similar to the one shown in Fig. 2 is provided in this section. The dimensional parameters of the robot are listed in Table I, where the left-superscript ${}^0(\cdot)$ indicates that the vector is expressed in the global (fixed) frame F_0 and ${}^e(\cdot)$ indicates that it is in the end-effector (moving) frame F_e .

TABLE I DIMENSIONS OF THE EXAMPLE CABLE ROBOT (UNIT: M)

Position vector	x	y	z	Position vector	x	y	z
${}^0 \mathbf{a}_1$	-0.5	0.00	-0.5000	${}^e \mathbf{b}_1$	0.0000	0	-0.1250
${}^0 \mathbf{a}_2$	-0.5	0.00	0.5000	${}^e \mathbf{b}_2$	0.0000	0	0.1250
${}^0 \mathbf{a}_3$	0.5	0.00	0.5000	${}^e \mathbf{b}_3$	0.0000	0	0.1250
${}^0 \mathbf{a}_4$	0.5	0.00	-0.5000	${}^e \mathbf{b}_4$	0.0000	0	-0.1250
${}^0 \mathbf{a}_5$	-0.2	0.05	-0.3464	${}^e \mathbf{b}_5$	-0.0625	1	-0.1083
${}^0 \mathbf{a}_6$	-0.2	0.05	0.3464	${}^e \mathbf{b}_6$	-0.0625	1	0.1083
${}^0 \mathbf{a}_7$	0.4	0.05	0.0000	${}^e \mathbf{b}_7$	0.1250	1	0.0000

The workspace was generated by choosing a large number of equally distributed end-effector poses in a predefined sampling space including the entire workspace and then checking each of the poses using the method described in Section IV. The workspace is graphically represented in Figs. 5-8. Figs. 5&6 show the workspace in x-y-z subspace while the end-effector is locked to an orientation of $(\theta_y, \theta_x, \theta_z) = (0,0,0)$, where $(\theta_y, \theta_x, \theta_z)$ represent the three 213 Euler angles of the end-effector with respect to the base frame. Figs. 7&8 display the workspace in terms of the Euler angles when the end-effector's position is fixed at $(x,y,z) = (0,0,0)$ in the base frame. It is interesting to notice that the workspace shown in Fig. 5 is convex and that in Fig. 7 is concave in topology. After having generated many different workspaces, it has been noticed that the force-closure workspace usually has a concave shape. The workspace shown in Fig. 4 is a very special case when all the orientation angles are zero. It will become concave as long as one of the orientation angles becomes nonzero. Fig. 9 shows how the workspace in x-y-z subspace changes its size (measured by volume) with respect to the variation of each of the three Euler angles. Obviously, the maximum workspace is achieved when the end-effector has an orientation of $(\theta_y, \theta_x, \theta_z) = (0,0,0)$. The volume of the workspace reduces nonlinearly with the increase of the end-effector orientation. For example, the size of the workspace reduces almost to 80% of its maximum value if the end-effector rotates $\pm 20^\circ$ about the z axis and 60% if the end-effector rotates $\pm 20^\circ$ about the x or y axis. This means that the cable-robot based HIL simulator shown in Fig. 1 should not be used to simulate a contact dynamics motion with a large relative orientation between the two simulated objects. This will not be a problem for the intended purpose of the simulator because, for the reliability and safety of a space mission, a real docking operation between two flying satellites must be controlled within an envelope of just a few degrees [19]. Even a possible bounce resulting from a physical impact during docking must also be within a small angle. Therefore, such a workspace can meet the usual requirements of simulating satellite docking and on-orbit servicing.

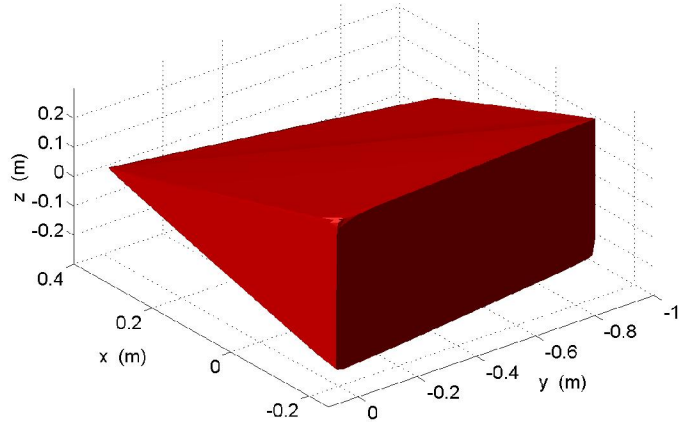


Fig. 5 Workspace when the end-effector's orientation is fixed.

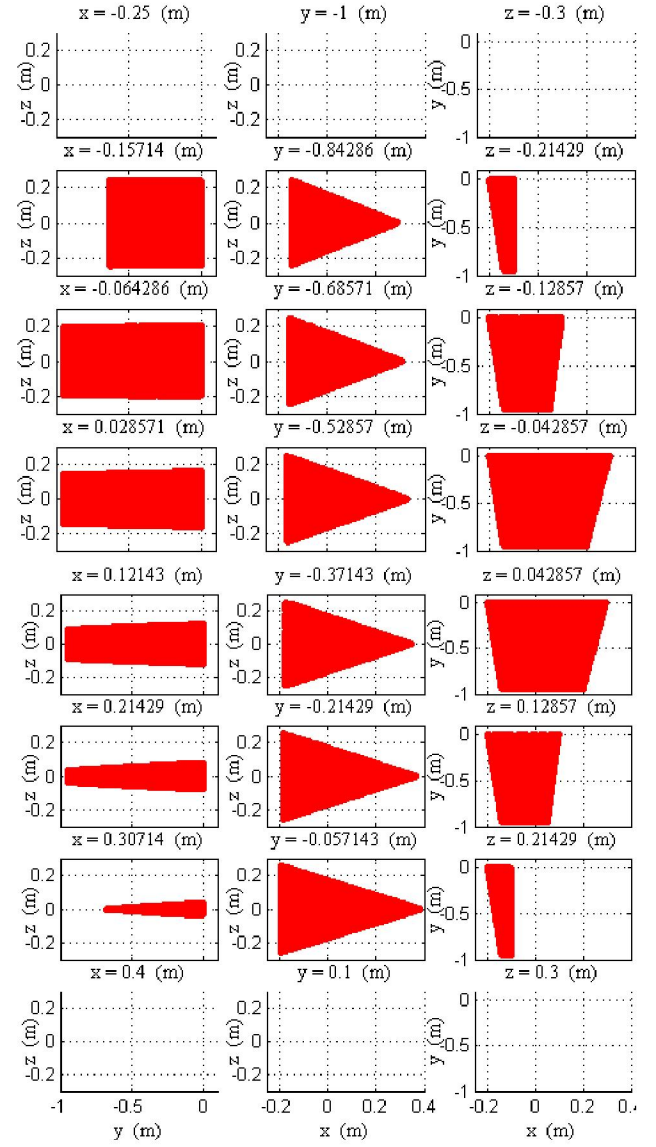


Fig. 6 Slices of the workspace (in Fig. 5) along the x, y, and z axes.

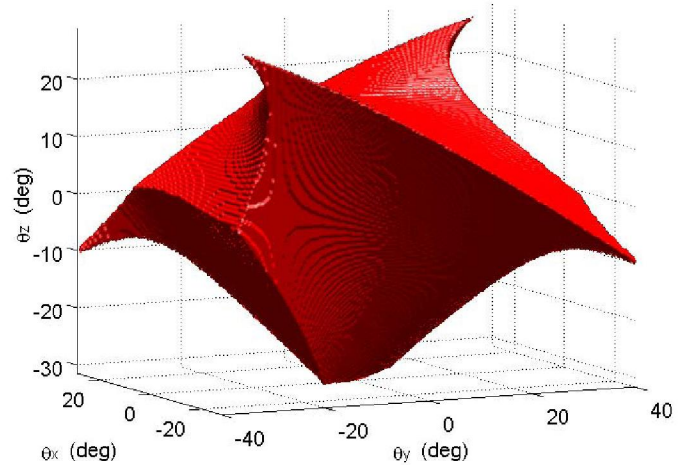


Fig. 7 Workspace when the end-effector's position is fixed.

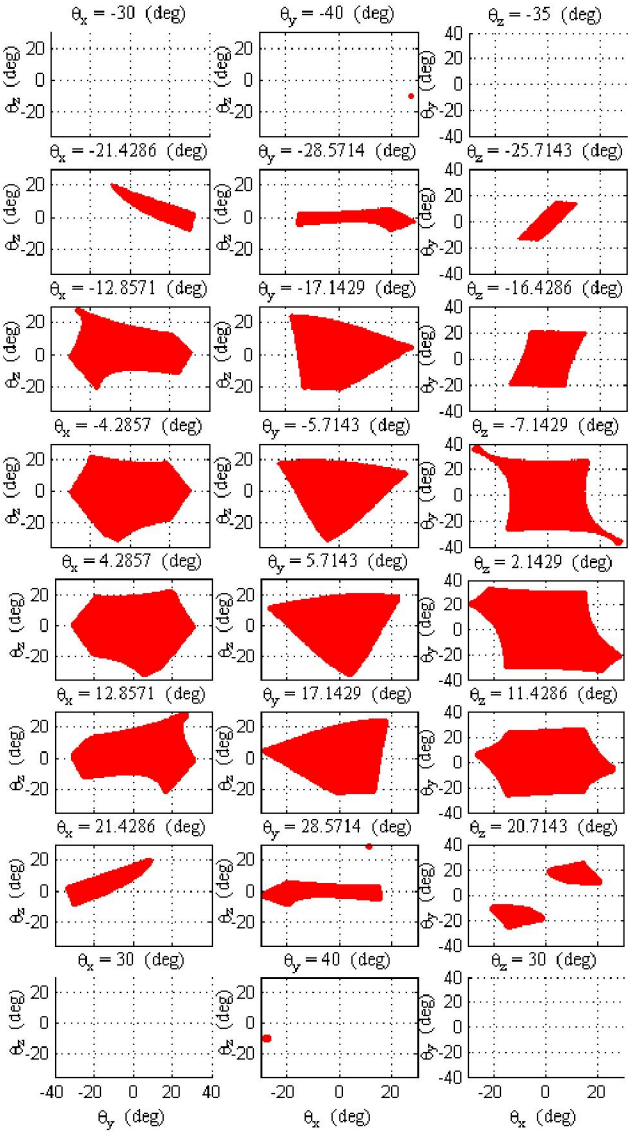


Fig. 8 Slices of workspace (in Fig. 7) along the θ_x , θ_y , and θ_z axes.

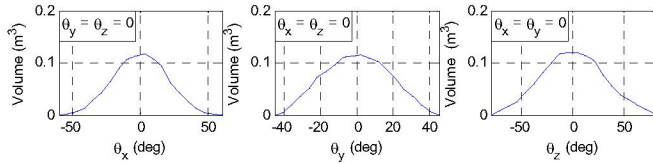


Fig. 9 Volume of the workspace (with fixed end-effector orientation such as the one shown in Fig. 5) vs the fixed end-effector orientation

VI. CONCLUSIONS

A force-closure workspace of a class of 6-DOF cable robots is defined and studied. Such a type of workspace allows not only any external wrench but also any dynamic motion of the end-effector and hence, it is the most desirable (or non-restricted) workspace for the intended application of the cable robot, namely, dynamic simulation of low-speed impact-contact operations of space systems, because such an

application requires the robot to have a large spectrum of motion state and external wrench. A systematic method of checking whether or not a given end-effector's pose is inside the workspace was introduced. Based upon this method, the shape, boundary, and volume of the workspace of a 6-DOF cable robot are determined and graphically displayed with a discussion about the workspace volume.

REFERENCES

- [1] S. Ananthakrishnan, R. Teders, and K. Alder, "Role of estimation in real-time contact dynamics enhancement of space station engineering facility", *IEEE Robotics and Auto. Mag.*, 1996, pp.20-28.
- [2] J.-C. Piedboeuf; J. De Carufel; F. Aghili; and E. Dupuis, "Task verification facility for the Canadian special purpose dexterous manipulator", *Proc. IEEE Int. Conf. on Robotics and Auto.*, Vol.3, 1999, pp.1077-1083.
- [3] R. Krenn and B. Schaefer, "Limitations of hardware-in-the-loop simulations of space robotics dynamics using industrial robots", *European Space Agency, ESA SP*, 1999, pp.681-686.
- [4] R. Verhoeven and M. Hiller, "Estimating the controllable workspace of tendon-based Stewart platforms", *Proc. 7th. Int. Symp. Advances Robot Kinematics*, Portoroz, Slovenia, 2000, pp. 277-284.
- [5] G. Barrette and C. Gosselin, "Determination of the dynamic workspace of cable-driven planar parallel mechanisms", *ASME Journal of Mechanical Design*, Vol.127, 2005, pp.242-248.
- [6] I. Ebert-Uphoff and P. A. Voglewede, "On the Connections Between Cable-Driven Robots, Parallel Manipulators and Grasping", *Proc. of IEEE Int. Conf. on Robotics & Auto.*, New Orleans, LA, Apr 2004, pp.4521-4526
- [7] P. Bosscher and I. Ebert-Uphoff, "Wrench-based Analysis of Cable-Driven Robots", *Proc. of IEEE Int. Conf. on Robotics & Auto.*, New Orleans, LA, April 2004, pp.4950-4955.
- [8] J. Pusey, A. Fattah, S.K. Agrawal, and E. Messina "Design and workspace analysis of a 6-6 cable-suspended parallel robot", *Mechanisms and Machine Theory*, Vol.39, No.7, 2004, pp.761-778.
- [9] R.L. Williams II, J.S. Albus, and R.V. Bostelman, "3D cable-based Cartesian metrology system", *J. of Robotic Systems*, Vol.21, No.5, 2004, pp.237-257.
- [10] A. Ming and T. Higuchi, "Study on multiple degree-of-freedom positioning mechanism using wires (part 1)", *International Journal of the Japan Society of Precision Engineering*, Vol. 28, No. 2, 1994, pp. 131-138.
- [11] M. Gouttefarde and C. Gosselin, "Analysis of the Wrench-Closure Workspace of Planar Parallel Cable-Driven Mechanisms", *IEEE Transactions on Robotics*, Vol. 22, No. 3, 2006, pp. 434-445.
- [12] O. Ma and X. Diao, "Dynamics analysis of a cable-driven parallel manipulator for hardware-in-the-loop dynamic simulation", *Proc. of the 2005 IEEE/ASME Int. Conf. on Advanced Intelligent Mechatronics (AIM 2005)*, 24-28 July, 2005, Monterey, CA, pp.837-842.
- [13] S. Kawamura, H. Kino, and C. Won, "High-speed manipulation by using a parallel wire-driven robots", *Robotica*, Vol.18, pp.13-21, 2000.
- [14] V.-D. Nguyen, "Constructing force-closure grasps", *The Int. J. of Robotics Research*, Vol. 7, No.3, 1988, pp.3-16.
- [15] M.R. Cutkosky, "On grasp, choice, grasp model, and the design of hands for manufacturing tasks", *IEEE Trans. On Robotics and Auto.*, Vol.5, No.3, 1989, pp.269-279.
- [16] G. Yang et al, "Kinematic design of a 7-DOF cable-driven humanoid arm: a solution-in-nature approach", *Proc. of the 2005 IEEE/ASME Int. Conf. on Advanced Intelligent Mechatronics (AIM 2005)*, 24-28 July, 2005, Monterey, CA, pp.444-449.
- [17] R. Murray, Z. Li, and S.S. Sastry, *A Mathematical Introduction to Robotic Manipulation*, CRC Press, 1994.
- [18] E. Stump and V. Kumar, "Workspace delineation of cable-actuated parallel manipulators", *ASME International Design Engineering Technical Conference*, Salt Lake City, UT, 2004.
- [19] W. Fehse, *Automated Rendezvous and Docking of Spacecraft*, Cambridge Univ. Press, London, 2003.